

Nonlinear endomicroscopy using a double-clad fiber coupler

Hongchun Bao,¹ Seon Young Ryu,² Byeong Ha Lee,^{3,4} Wei Tao,¹ and Min Gu^{1,5}

¹Centre for Micro-Photonics, Faculty of Engineering & Industrial Sciences, Swinburne University of Technology, Hawthorn, Victoria 3122, Australia

²Division of Instrument Development, Korea Basic Science Institute, 113 Gwahangno, Yuseong-gu, Daejeon 305-333, Korea

³Department of Information and Communications, Gwangju Institute of Science and Technology, 1 Oryong-dong, Buk-gu, Gwangju, 500-712, Korea

⁴leebh@gist.ac.kr

⁵mgu@swin.edu.au

Received December 2, 2009; revised February 8, 2010; accepted February 19, 2010;
posted March 3, 2010 (Doc. ID 120614); published March 26, 2010

A double-clad fiber coupler is developed to be used in two-photon-excited fluorescence endomicroscopy to replace a dichroic mirror and separate the fluorescence signal from the excitation laser beam. With the double-clad fiber coupler, the endomicroscope becomes more compact, easier to be aligned, and more stable in alignment. The double-clad fiber coupler can transmit 62% of the excitation laser beam through the core. The fluorescence collection efficiency of the double-clad fiber coupler is 34%, which is, to the best of our knowledge, the highest fluorescence collection efficiency achieved by couplers used in two-photon-excited fluorescence endomicroscopes. As a result, the contrast of endomicroscopy imaging is enhanced. © 2010 Optical Society of America

OCIS codes: 110.6880, 180.2520.

Two-photon-excited fluorescence (TPF) endomicroscopy using a flexible thin optical fiber and a miniaturized probe can image an area in a very tight space with high resolution, where a bulky microscope cannot reach [1–5]. The endomicroscope uses near-IR ultrashort optical pulses for imaging, which allows three-dimensional imaging further in the sample as compared with regular confocal imaging [6,7]. Therefore it provides a useful tool for *in vivo* imaging and real-time monitoring of targets with minimal invasion [8,9].

It is essential that a TPF endomicroscope is compact and easily maintains alignment for immediate use and stable during imaging. In TPF imaging, reflected light from the excitation laser needs to be separated from the fluorescence [10,11]. Normally a dichroic mirror is used for this separation. However, such a system consumes time for alignment and environmental conditions easily affect its performance. It needs an extra green light laser for the alignment of the endoscope using a dichroic mirror. Any vibration at transportation or operation of an endomicroscope can change the position of a dichroic mirror and degrade the system alignment. Therefore an endomicroscope has to be compact for clinical use. Single-mode couplers and double-clad photonic crystal fiber (DCPCF) couplers have been investigated in endomicroscopy systems for easy alignment [12–16]. However, the fluorescence collection efficiency of a single-mode fiber is low, and the endomicroscope suffers from a low signal to noise ratio. A DCPCF increases the fluorescence signal collection efficiency. However, the confinement of light in the core and the inner cladding depend on the hole structure of the DCPCF. Among all the excitation light transmitting in the DCPCF, only 30% can be successfully transmitted in the core [11], and 70% of the excitation light is lost at

the inner cladding and cannot be efficiently used for the excitation of fluorescence signal [11]. In addition, the DCPCF coupler can transmit only 2.8% of the total fluorescence signal owing to its low-cross coupling ratio of the inner cladding [16], although it has a fluorescence collection efficiency as high as 98% within its NA.

In this Letter, a double-clad fiber coupler (DCF) is developed for separating the fluorescence signal from the excitation laser beam. The DCF coupler can confine 62% of the total transmitted excitation light into the core, which is twice as much as the DCPCF coupler [11]. The fluorescence signal collection efficiency of the DCF coupler is 34% and 12 times higher than that of the DCPCF coupler. For the same excited fluorescence signal from a sample, the DCF coupler enhances the signal-to-noise ratio and the contrast of imaging by 12 times compared with the DCPCF coupler.

Figure 1 illustrates a DCF and the DCF coupler. A DCF (Fibercore, SMM900 3.6/105/125 μm core/inner/outer cladding) is used for fabrication of a DCF coupler. Previously DCF couplers were developed using conventional methods [17], the fused biconical tapered (FBT) method [16,18] or the side-polishing method [19], and the simple contact method [20]. In this work the DCF coupler is fabricated with the FBT method. As an 800 nm excitation laser beam is coupled into port 3 of the DCF coupler, the center part of port 1 [Fig. 1(b)] has a high light intensity, while the surrounding part of port 1 has weak light. The elongated center spot shown in Fig. 1(b) is due to the saturation of the imaging camera. On the contrary, the center of port 4 [Fig. 1(c)] is dark, and the surround area is bright. Therefore the DCF coupler can transmit the excitation laser beam through the core from port 3 to port 1 with little loss of light to the

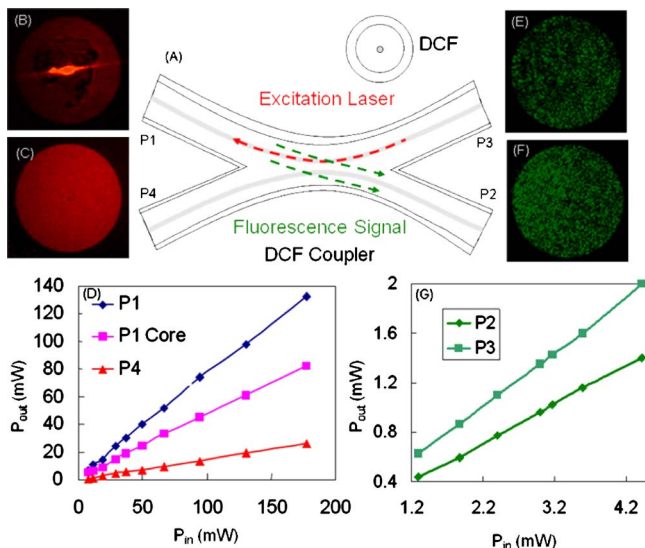


Fig. 1. (Color online) (A) Schematic structure of a four-port DCF coupler and a DCF. (B), (C) Light output patterns at port 1 and port 4 for an 800 nm femtosecond laser beam coupled to port 3 of the DCF coupler. (D) Output power at port 1, in the core of port 1 and at port 4 versus the input power at port 3. (E), (F) Light output patterns at port 3 and port 2 for a 532 nm laser beam coupled to port 1 of the DCF coupler. (G) Output power at port 2 and port 3 versus the incident power of the DCF coupler.

arm at port 4, and the light leaking to port 4 is mainly from the inner cladding. 90% of the input excitation laser beam can be coupled into the DCF coupler. 85% of the light propagates to port 1, and 15% propagates to port 4 [Fig. 1(d)]. 62% of the light can be used for the generation of TPF signal [Fig. 1(d)]. This is ideal for delivering the laser beam in a compact nonlinear endomicroscope.

The fluorescence signal, which is in the visible spectral range, is collected from port 1 to port 2 by the DCF coupler. Figs. 1(e) and 1(f) illustrate the light patterns at port 2 and port 3 when a 532 nm cw green light beam is coupled to port 1. Port 2 has bright light around the inner cladding. 34% of the incident green light can be cross coupled to port 2 [Fig. 1(g)]. The DCF has a large visible light collection efficiency, which, to our knowledge, is the highest among all the couplers ever used in TPF endomicroscopes. The fluorescence collection efficiency can be further increased by increasing the fusion strength of the DCF coupler. However, a strongly fused DCF coupler also leads to the increase of the loss of the excitation laser beam transmitting through the core. Therefore the fusion strength is chosen by maximizing cross coupling at visible light before the loss of the excitation light at the core starts to increase.

A compact endoscopic system is displayed in Fig. 2. The excitation laser beam is from a Ti:sapphire laser that generates 80 MHz 100 fs optical pulses. The optical pulses are first prechirped by a pair of gratings. The negative frequency chirp that the optical pulses gain by propagating through the gratings is used to compensate for the normal chromatic dispersion, which they gain later transmitting through the DCF coupler and a DCF. The prechirped

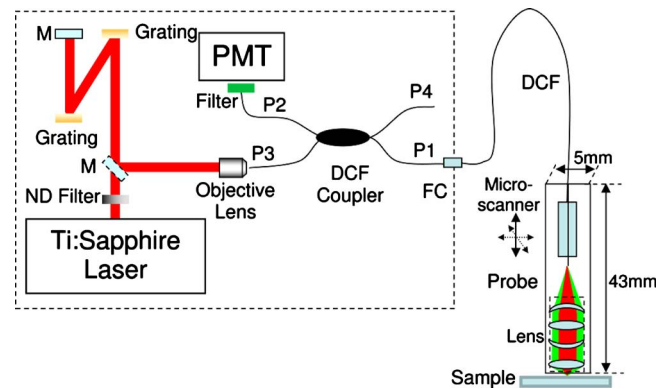


Fig. 2. (Color online) TPF endomicroscopy using the DCF coupler. FC, fiber connector; M, mirror; ND, neutral density.

optical pulses are coupled into port 3 of the DCF coupler. Port 1 is connected to a 2 m DCF through a fiber connector (FC). At the end of the DCF, a miniaturized probe is attached to the DCF [2,21,22]. Inside the probe, a microscanner scans the DCF tip line by line for imaging [2,21,22]. The microscanner can also move the DCF and the objective lens forward and backward to achieve three-dimensional (3D) imaging with an axial scanning range of 250 μm . A multiple element objective lens focuses excitation laser beam to samples and collects the TPF signal from the samples to the DCF. The object NA of the lens is same as the core NA of the DCF of 0.2, and the image NA is 0.35. Therefore the magnification of the lens is 1.75. The field of view for imaging is 475 $\mu\text{m} \times 475 \mu\text{m}$, and the useful fiber scanning range is 831 $\mu\text{m} \times 831 \mu\text{m}$. The fluorescence signal is separated from the excitation laser beam by the DCF coupler and detected by a photomultiplier tube after being filtered by a 3-mm-thick BG18 glass filter (Schott). With the DCF coupler in TPF endomicroscopy to replace a dichroic mirror, the endomicroscope requires minimal alignment and can be ready for imaging with minimal preparation time. Furthermore, the alignment is more stable during imaging.

Figure 3 illustrates clear sectioning images of the microspheres at different depths with a full field of view of 475 $\mu\text{m} \times 475 \mu\text{m}$. The excitation power at

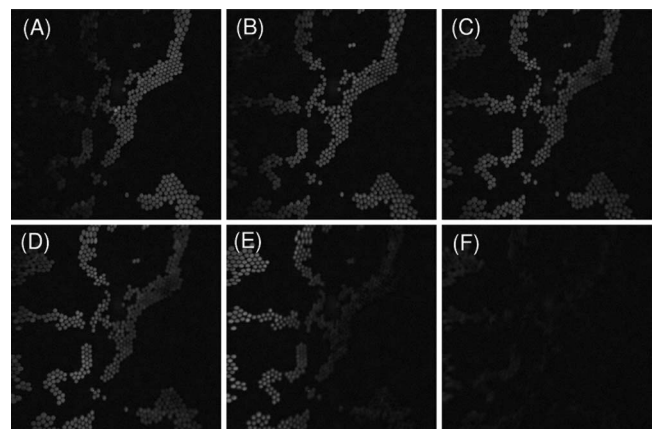


Fig. 3. Set of TPF images of 10 μm diameter fluorescent microspheres with an axial step of 4 μm .

the sample is 16 mW. For the bulky endomicroscope using a dichroic mirror [2], the same brightness of imaging needs 9 mW of the excitation laser beam. A higher excitation laser power level is required for the compact endomicroscope.

Figure 4(a) shows the image of a mouse kidney after injected fluorescein intravenously. The excitation power at the sample is 18 mW. The compact endomicroscope clearly displays the image of the biological sample. To understand the resolution of the endomicroscope, $1\ \mu\text{m}$ fluorescence microspheres are imaged [Fig. 4(b)], and the average fluorescence intensity profile of the microspheres is displayed in Fig. 4(c). The FWHM of the average intensity profile is $1\ \mu\text{m}$. Therefore, the lateral resolution of the TPF endomicroscope is better than $1\ \mu\text{m}$. The axial resolution of the endomicroscope is measured by scanning a thin layer of polymer with 4 diethylaminobenzylidene-malononitrile (DABM) as a dye along the z direction [Fig. 4(d)]. The FWHM of the intensity profile is $14\ \mu\text{m}$. Thus the axial resolution of the endomicroscope is better than $14\ \mu\text{m}$. Compared with the endomicroscope using a dichroic mirror [2], the DCF coupler has no obvious effect on the lateral and axial resolutions.

In conclusion, compact TPF endomicroscopy is developed using a DCF coupler to replace a bulky beam splitter. With the DCF coupler, the endomicroscope can be quickly aligned and is fast to be ready for imaging, which is important for the practical use of endomicroscopy. The DCF coupler has a large fluorescence collection efficiency of 34%, which helps to

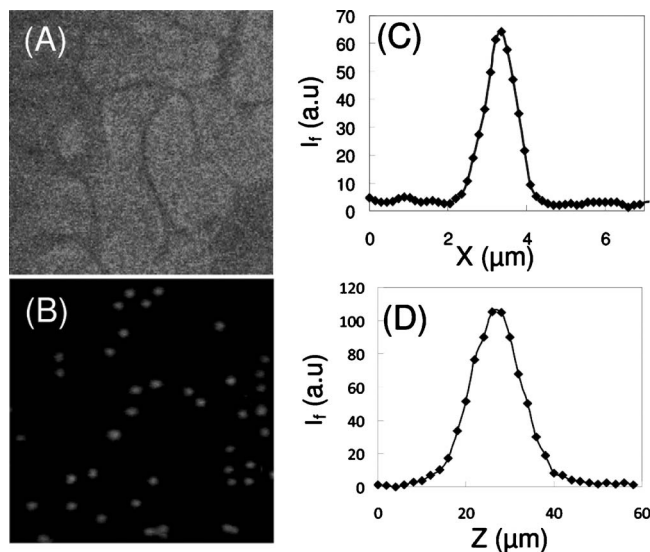


Fig. 4. (A) TPF images of a mouse kidney. Size of the image: $150\ \mu\text{m} \times 150\ \mu\text{m}$. (B) Image of $1\ \mu\text{m}$ diameter fluorescent microspheres. Size of the image: $30\ \mu\text{m} \times 30\ \mu\text{m}$. (C) Average fluorescence intensity profile of the microspheres. (D) Axial response of the TPF signal from a thin layer of DABM dye.

enhance the signal-to-noise ratio of endomicroscopy imaging. The lateral and axial resolution of the nonlinear endomicroscope is better than $1\ \mu\text{m}$ and $14\ \mu\text{m}$, respectively. The development of compact TPF endomicroscopy is an important step for nonlinear endomicroscopy toward all fiber nonlinear endomicroscopy.

The authors thank the Australian Research Council and the Korea Science and Engineering Foundation (KOSEF) grant funded by the Korea government (MEST) (No. R01-2007-000-20821-0) for their supports and acknowledge that the double-clad fiber coupler used this paper was made at Gwangju Institute of Science and Technology. The biological samples were provided by Dr. Rita Busuttill and Ms. Alexandria McGearey from Peter MacCallum Cancer Centre, Australia.

References

1. D. Yelin, I. Rizvi, W. M. White, J. T. Motz, T. Hasan, B. E. Bouma, and G. J. Tearney, *Nature* **443**, 765 (2006).
2. H. Bao, J. Allen, R. Pattie, R. Vance, and M. Gu, *Opt. Lett.* **33**, 1333 (2008).
3. W. Jung, S. Tang, D. T. McCormic, T. Xie, Y. Ahn, J. Su, I. V. Tomov, T. B. Krasieva, B. J. Tromberg, and Z. Chen, *Opt. Lett.* **33**, 1324 (2008).
4. F. Helmchen, M. S. Fee, D. W. Tank, and W. Denk, *Neuron* **31**, 903 (2001).
5. B. A. Flusberg, E. D. Cocker, W. Piyawattanametha, J. C. Jung, E. L. M. Cheung, and M. J. Schnitzer, *Nat. Methods* **2**, 941 (2005).
6. F. Helmchen and W. Denk, *Nat. Methods* **2**, 932 (2005).
7. P. Theer, M. T. Hasan, and W. Denk, *Opt. Lett.* **28**, 1022 (2003).
8. M. E. Llewellyn, R. P. J. Barretto, S. L. Delp, and M. J. Schnitzer, *Nature* **454**, 784 (2008).
9. K. König, A. Ehlers, I. Riemann, S. Schenkl, R. B. Ckle, and M. Kaatz, *Microsc. Res. Tech.* **70**, 398 (2007).
10. H. Bao and M. Gu, *Opt. Express* **17**, 10098 (2009).
11. H. Bao and M. Gu, *Opt. Lett.* **34**, 148 (2009).
12. D. Bird and M. Gu, *Opt. Lett.* **27**, 1031 (2002).
13. L. Fu and M. Gu, *Opt. Express* **16**, 5000 (2008).
14. D. Bird and M. Gu, *Opt. Lett.* **28**, 1552 (2003).
15. L. Fu, X. Gan, and M. Gu, *Opt. Lett.* **30**, 385 (2005).
16. L. Fu and M. Gu, *Opt. Lett.* **31**, 1471 (2006).
17. S. Y. Ryu, H. Y. Choi, J. Na, B. H. Lee, and E. S. Choi, *Opt. Lett.* **33**, 2347 (2008).
18. B. P. Pal, P. R. Chaudhuri, and M. R. Shenoy, *Fiber Integr. Opt.* **22**, 97 (2003).
19. L. Wang, H. Y. Choi, Y. Jung, B. H. Lee, and K. Kim, *Opt. Express* **15**, 17681 (2007).
20. S. Y. Ryu, H. Y. Choi, M. J. Ju, J. Na, W. J. Choi, and B. H. Lee, *J. Opt. Soc. Korea* **13**, 310 (2009).
21. R. Kiesslich, P. R. Galle, and M. F. Neurath, *Atlas of Endomicroscopy* (Springer, 2008).
22. M. Goetz, C. Fottner, E. Schirmacher, P. Delaney, S. Gregor, C. Schneider, D. Strand, S. Kanzler, B. Memadathil, E. Weyand, M. Holtmann, R. Schirmacher, M. M. Weber, M. Anlauf, G. Klöppel, M. Vieth, P. R. Galle, P. Bartenstein, M. F. Neurath, and R. Kiesslich, *Endoscopy* **39**, 350 (2007).